The Royal Society

Multiple groups of orientation-selective visual mechanisms underlying rapid orientated-line detection

David H. Foster[1*] **and Stephen Westland**[2]

[1]*Department of Vision Sciences, Aston University, Birmingham B4 7ET, UK* (d.h.foster@aston.ac.uk)
[2]*Department of Communication and Neuroscience, University of Keele, Staffordshire ST5 5BG, UK*

Visual search for an edge or line element differing in orientation from a background of other edge or line elements can be performed rapidly and effortlessly. In this study, based on psychophysical measurements with ten human observers, threshold values of the angle between a target and background line elements were obtained as functions of background-element orientation, in brief masked displays. A repeated-loess analysis of the threshold functions suggested the existence of several groups of orientation-selective mechanisms contributing to rapid orientated-line detection; specifically, coarse, intermediate and fine mechanisms with preferred orientations spaced at angles of approximately 90°, 35°–50° and 10°–25°, respectively. The preferred orientations of coarse and some intermediate mechanisms coincided with the vertical or horizontal of the frontoparallel plane, but the preferred orientations of fine mechanisms varied randomly from observer to observer, possibly reflecting individual variations in neuronal sampling characteristics.

Keywords: preattentive vision; filters; orientation tuning; cortex; visual search; oblique effect

1. INTRODUCTION

Of all the visual cues in a monochromatic static scene that might aid search for a target, one of the most effective is line or edge orientation (Beck & Ambler 1972; Treisman *et al*. 1977; Sagi & Julesz 1985). A line element differing sufficiently in orientation from a background of other line elements (see figure 1) can be detected in a display exposed for a few tens of milliseconds before being masked: the target element is said to 'pop out' (Treisman 1985; Nothdurft 1991; Wolfe 1992). Under suitable conditions (Javadnia & Ruddock 1988; Doherty & Foster 1995), the level of detection performance is found to depend little on the number of elements in the display, and the visual mechanisms involved may be assumed to act in parallel over the visual field (Treisman & Gelade 1980; Sagi & Julesz 1985). Because the task does not require scanning of the display, it is sometimes considered to be preattentive (Neisser 1967), involving primarily the early stages of visual processing (Julesz & Schumer 1981; Bergen & Julesz 1983; Treisman 1985). Such processing, although inferred from laboratory experiments with simple, geometrical stimuli, almost certainly occurs in more naturalistic, real-world situations (Wolfe 1994).

What kind of visual mechanisms underlie rapid orientated-line detection? A clue is offered by an asymmetry in search performance (Treisman & Souther 1985): it is easier to find an obliquely orientated line element in a background of vertically orientated line elements than a vertically orientated line element in a background of obliquely orientated line elements (in the frontoparallel plane). More extensive, although sparsely sampled, data have been obtained on the threshold orientation difference between target and background elements as a function of background-element orientation, the 'orientation increment-threshold function'. This function, averaged over observers and sampled at 22.5° orientation intervals, was found to have minima when the background elements were vertical and horizontal. As is shown here, there are difficulties in accounting for this asymmetry in terms of the classical oblique effect, in which orientation acuity and similar measures are poorer along the oblique axes than along the vertical and horizontal axes. It can, however, be explained quantitatively with reference to two classes of broadband anisotropic mechanisms orientated along the vertical and horizontal, with half-widths at half-height of about 30° (Foster & Ward 1991). It has been suggested that the orientation-tuning functions of these mechanisms are closely matched to certain statistical components of real-world images (Baddeley & Hancock 1991).

Given the limited data available on the orientation increment-threshold function, it is not possible to conclude that these two orthogonal mechanisms are the only ones contributing to rapid orientated-line detection; the aim of the present study, therefore, was to explore the involvement of more finely tuned mechanisms in the performance of individual human observers.

To this end, orientated-line detection in brief, masked displays was determined at 5° intervals of target and background line-element orientation for ten observers.

*Author for correspondence.

Received 20 April 1998 *Accepted* 11 May 1998

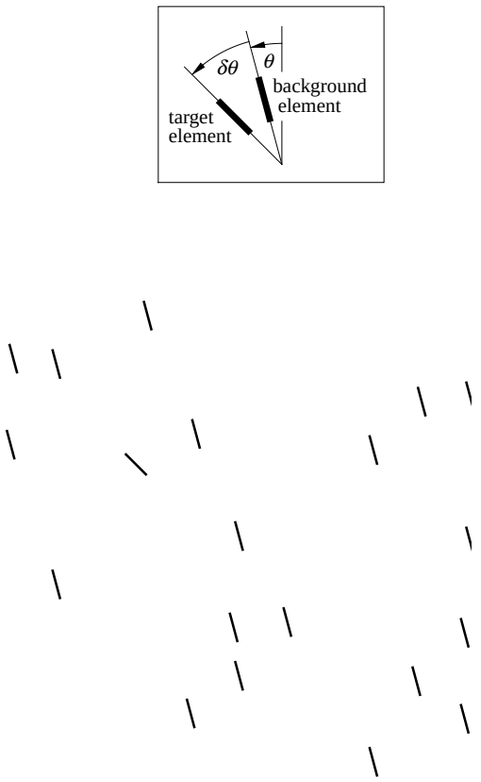

Figure 1. Typical stimulus display (with contrast reversed). The line elements, each subtending 1° at the eye, were distributed randomly over a field subtending 20° × 20° visual angle. They all had the same orientation, except for a target line element, which was present in 50% of trials. When there was no target an additional background element was introduced so that target and non-target displays had the same number of elements. The duration of the display was 40 ms; it was followed by a blank field lasting 60 ms, and then by a masking field lasting 500 ms. Inset: the orientation θ of the background elements was drawn randomly from the range 0°, 5°, . . ., 175°, and the difference $\delta\theta$ in angle between target and background elements was drawn randomly from the range 5°, 10°, . . ., 40°.

From these data, orientation increment-threshold functions were obtained, which were then analysed by a method based on repeated loess (Cleveland 1993). This analysis suggested the existence of several groups of orientation-selective mechanisms contributing to orientated-line detection: coarse and intermediate mechanisms with preferred orientations spaced at angles of *ca.* 90° and 35°–50°, respectively, and fine mechanisms with preferred orientations spaced at *ca.* 10°–25°. The preferred orientations of the coarse and some intermediate mechanisms coincided with the vertical or horizontal, in contrast to the preferred orientations of the fine mechanisms, which varied randomly from observer to observer. When the interval between the line-element display and the mask was increased for two of the observers, the apparent activity of the coarse mechanisms diminished with little or no change in the activity of the intermediate or fine mechanisms.

2. METHODS

(a) *Stimuli*

Figure 1 shows a typical line-element display (with contrast reversed). It consisted of 20 identical line elements, each line element subtending 1° by *ca.* 0.1° at the eye. The elements were distributed randomly (Meigen *et al.* 1994) over a field subtending 20° × 20° visual angle, but not allowed to fall so closely together that they formed new perceptual features. The density of the elements in the field was probably too low for highly local orientation contrast to influence performance (cf. Sagi & Julesz 1987; Westheimer 1990). All the line elements in the display had the same orientation, except for the target, which was present in 50% of trials. When the target was absent it was replaced by a background element so that target and non-target displays had the same number of elements. The orientations of the target and background elements were chosen randomly. The location of the target was also chosen randomly, but was constrained to fall within an imaginary annulus of radius 3°–8° to reduce the effects of retinal inhomogeneity (Sagi & Julesz 1987). The duration of the line-element display was 40 ms. It was followed by a blank field lasting 60 ms, and then by a masking field lasting 500 ms, the purpose of the latter being to limit the effective display duration (i.e. the time available for inspection of the fading afterimage of target and background elements). The mask consisted of 20 patches of four randomly orientated line elements, with the arrangement of the elements differing from patch to patch and each patch covering one of the previously displayed line elements. The stimulus time-course was chosen on the basis of previous experiments (Foster & Ward 1991; Doherty & Foster 1996*b*).

(b) *Apparatus*

Stimuli were presented on the screen of a cathode-ray tube (CRT) (Hewlett-Packard, USA; Type 1317A, green P31 phosphor, measured 90%–10% decay time less than 100 μs, rise time less than decay time) controlled by a true-line vector-graphics generator (Sigma Electronic Systems, UK; QVEC 2150) and additional digital-to-analogue converters, in turn controlled by a laboratory computer. (No difference was found between performances obtained with green and fast white phosphors.) The screen was refreshed at intervals of 20 ms. This temporal structure was not visually detectable by the observer.

This system produced very-high-resolution line-element displays in which individual line elements were defined with end-point (linear) resolutions of 1 part in 1024 over an imaginary square patch of side 1.25 cm. Each patch was located with precision of 1 part in 4096 over the 17 inch (43 cm) CRT screen. The accuracy of local positioning was verified with a travelling microphotometer. Orientation accuracy was differentially better than 0.2° and absolutely better than 0.5°. The intensity of the line elements did not vary with their orientations.

As a control on the fidelity of the stimuli presented in the experiment, they were photographed at their display durations and then measurements were made on the photographic prints. Before each experimental session the CRT was allowed to warm up for 20 min and its spatial calibration was then verified by aligning a test image against a transparent template that was placed over the screen.

(c) *Procedure*

The display was viewed binocularly by the observer at 50 cm through a view-tunnel that produced a uniformly illuminated,

white background, of luminance *ca.* 40 cd m^{-2}, on which the line-element stimuli appeared superimposed. The luminance of the line elements was set by the observer at the beginning of each experimental session to ten times threshold on the uniform background (a 1-log-unit neutral-density filter was placed between the CRT screen and view-tunnel, thereby leaving the background unattenuated; the luminance of the attenuated line-element stimuli was set to threshold on the background; then the neutral density filter was removed). This luminance level was not critical: variations in the increment-threshold function of the kind reported here have been obtained with a range of luminance contrasts (Doherty & Foster 1996*a*).

The observer started each trial and responded as to whether a target was present by pressing button switches connected to the computer. Fresh random displays (and masks) were generated in every trial. The orientation θ of the background elements was drawn from the range 0°, 5°, . . ., 175°(0° vertical in the frontoparallel plane), and the difference $\delta\theta$ in angle between the target element and the background elements was drawn from the range 5°, 10°, . . ., 40° (with θ and $\delta\theta$ being measured in the same direction, positive anticlockwise (see inset figure 1); the direction, anticlockwise or clockwise, was chosen randomly from trial to trial). The ordering of θ and $\delta\theta$ values over the complete sequence of trials performed by each observer was chosen randomly (with different random sequences for different observers). As values were not blocked, any potential confounding between the effects of target- and background-element orientation and the effects of testing order was thereby minimized (cf. Hirsch & Hylton 1982; Westheimer 1984).

Trials were performed in sessions lasting no more than 1 h. Each observer performed, on average, 13 000 trials over a period of several months. Observers were not given feedback. As there have been reports of learning in orientated-line-detection tasks (Karni & Sagi 1991; Schoups & Orban 1996; Ahissar & Hochstein 1997), the data were tested for evidence of practice effects. A small improvement in performance was found: thresholds over each observer's first 5000 trials were, on average, about 10% higher than over the remaining trials, although the effect did not reach significance ($t_9 = 1.36$, $p = 0.1$). This finding is consistent with the observation by Ahissar & Hochstein (1997) that learning in tasks with small orientation increments (similar to those used here) tends to be position specific, a condition avoided in the present study where the target was placed randomly within the prescribed region.

(d) *Subjects*

There were ten observers. Each had normal or corrected-to-normal vision (Snellen acuity 6/4–6/6 and optometrically verified astigmatism less than 0.25 dioptre). They were aged 19–30 years, and, except for one (co-author S.W.), they were unaware of the purpose of the experiment and were paid for their participation.

(e) *Data Analysis*

Target detection at each combination of background-element orientation θ and target increment $\delta\theta$ was summarized by the discrimination index d' from signal-detection theory (Green & Swets 1966). In essence, if HR is the detection hit rate, FAR the false-alarm rate, and Φ^{-1} the inverse of the cumulative unit normal distribution, then $d' = \Phi^{-1}(\mathrm{HR}) - \Phi^{-1}(\mathrm{FAR})$. In this way, d' linearizes and combines responses to target and non-target displays; furthermore, if certain conditions on the underlying psychophysical mechanisms are satisfied, then d' is independent of observer bias (Green & Swets 1966).

A graph of d' against $\delta\theta$ was thus obtained at each θ. Some graphs had both concave and convex sections, and a cubic curve g was therefore fitted. Fitting was by weighted least-squares and was constrained so that $g(0) = 0$. A cubic curve accounted adequately for the variance in the data (maximum $\chi^2 = 196$, d.f.=180, $p \geqslant 0.2$). For a selected criterion level of target detection defined by d' (e.g. 0.5), the corresponding threshold value $\Delta\theta$ of $\delta\theta$ was calculated from the fitted curve ($\Delta\theta$ being the value of $\delta\theta$ closest to zero such that, for the $d' = 0.5$ criterion, $g(\delta\theta) = 0.5$). The standard deviation of $\Delta\theta$ was estimated by a resampling (parametric bootstrap) method (Foster & Bischof 1991; Efron & Tibshirani 1993). Each threshold value $\Delta\theta$ was based on *ca.* 370 trials. The choice of criterion level of d' was constrained by two requirements: that the $\Delta\theta$ should be stable (i.e. have small standard deviations) and that the shape of the increment-threshold functions should be invariant under reasonable changes in d' (Foster & Ward 1991). For values of d' greater than about 0.8, one or other of these requirements was not satisfied.

Discrimination performances obtained with anticlockwise (θ,$\delta\theta$) and clockwise ($-\theta$, $-\delta\theta$) rotations were indistinguishable ($t_{359} = 1.28$, $p = 0.1$); responses were therefore pooled over the two directions. For any particular combination (θ',$\delta\theta'$), the combination (θ', $-\delta\theta'$) could be identified with (180°$-\theta'$, $\delta\theta'$).

As is shown later, the resulting increment-threshold functions appeared to have partly periodic structures at several orientation scales, and the question arose of how best to reveal them. A Fourier analysis of the increment-threshold functions would not, in itself, have served (Appendix Aa, which can be found at `http://www.pubs.royalsoc.ac.uk/publish/pro_bs/`), nor a principal-components analysis (Appendix Ab). As the functions have the form of a series with superimposed noise, it is possible to draw on methods of analysis developed for time-series problems (where 'time' may refer to time, spatial position, etc.). Repeated loess (Cleveland 1993) is a non-parametric statistical filtering procedure for decomposing a set of time-series-like data into several components by a process of progressive smoothing and differencing. The procedure, which uses locally weighted polynomial (quadratic) regression (Cleveland 1979; Fan & Gijbels 1996), involves no assumptions about the periodicity of the components and only very weak assumptions about their shape. Details of these assumptions and of how the repeated-loess procedure was implemented here are given in Appendix Ac and the results of several control measurements are given in Appendix B, which can be found at `http://www.pubs.royalsoc.ac.uk/publish/pro_bs/`.

3. DETECTION AT MULTIPLE ORIENTATION SCALES

Figure 2 shows superimposed orientation increment-threshold functions for line-element detection for the ten observers. The continuous lines connect threshold values $\Delta\theta$ of the difference $\delta\theta$ in orientation between target and background elements at each background-element orientation θ for a criterion level of target detection d' equal to 0.5. There is a rapid oscillation of $\Delta\theta$ with θ, which varies markedly from observer to observer, along with a more general underlying slow variation with a period of about 90°(cf. Foster & Ward 1991).

Analysing performance en bloc, as in figure 2, has limited value (Appendix Ab). Instead, observers' increment-threshold functions were analysed individually.

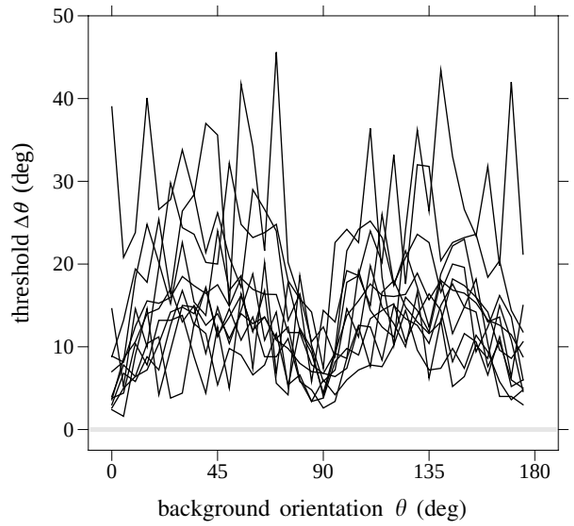

Figure 2. Orientation increment-threshold functions for line-element detection for ten observers. The continuous lines connect threshold values $\Delta\theta$ of the difference $\delta\theta$ in orientation between target and background elements at each background-element orientation θ ($\theta = 0°$ corresponds to the vertical in the frontoparallel plane).

Consider, by way of example, data from observer G.P.W. Figure 3 shows this observer's increment-threshold function and the results of the decomposition analysis (another example, for observer A.C., is shown in figure 6). In figure 3*a* the open symbols show threshold values $\Delta\theta$ plotted against background-element orientation θ for d'=0.5; the vertical bars indicate ±1 s.d., where sufficiently large. Values of $\Delta\theta$ varied from *ca.* 2° to *ca.* 20°, much larger and with a much larger range of variation than in classical orientation-acuity measurements with simple, relatively long-duration, unmasked stimuli (e.g. Andrews 1967; Westheimer & McKee 1977). As with other observers (figure 2), there is a combination of slow and more rapid variations of $\Delta\theta$ with θ. The question of the statistical significance of these variations is addressed systematically later.

Figure 3*b* shows the slowest-varying, that is, the coarsest, orientation component obtained from the repeated-loess decomposition of the increment-threshold function. Figure 3*c–e* shows progressively finer orientation components, distinguished by the number n of minima obtained at the scale or bandwidth h of smoothing (h coincides with the standard deviation of the wrapped Gaussian function weighting the local quadratic regression; Appendix Ac). At all scales there are departures from strict periodicity (see also figure 6).

The continuous curve passing through the data points in figure 3*a* is the sum of the components in figure 3*b–e*. This curve, although not a perfect fit, accounted adequately for the variance in the increment-threshold data in figure 3*a* ($\chi^2 = 8.98$, d.f.=9.74, $p = 0.5$, where d.f. was calculated from the trace of the matrix used to smooth the data (Hastie & Tibshirani 1990, p. 52)). The summed curve coincides with a low-pass-filtered version of the increment-threshold function (Appendix Aa).

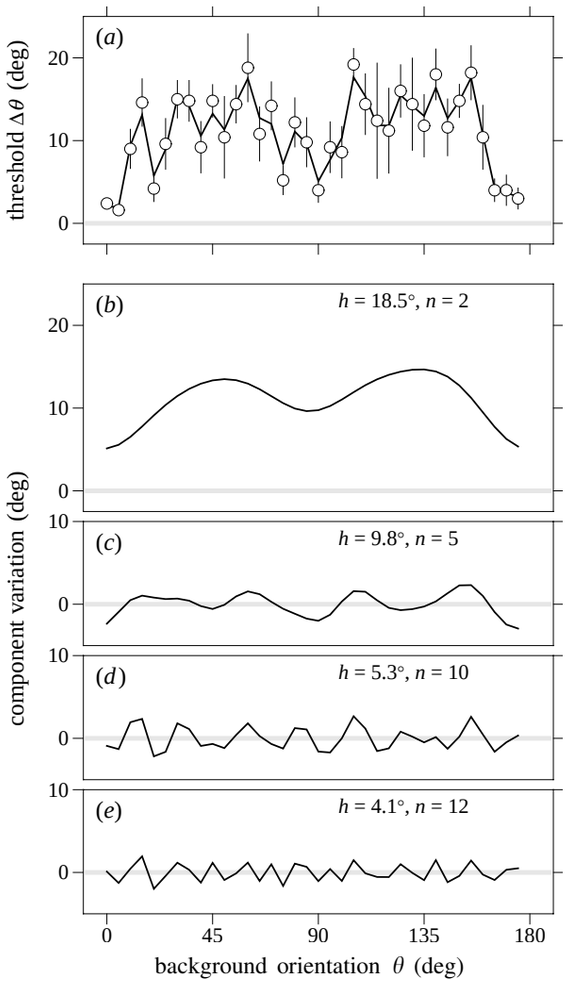

Figure 3. Individual orientation increment-threshold function and its decomposition into components obtained by a procedure based on repeated loess (Cleveland 1993). (*a*) Threshold value $\Delta\theta$ of the difference $\delta\theta$ in orientation between target and background elements (open symbols) plotted against background-element orientation θ. Vertical bars indicate ±1 s.d., where sufficiently large. (*b–e*) Coarsest orientation component and progressively finer components, distinguished by the number n of minima at the bandwidth h of smoothing. The continuous curve passing through the data points in (*a*) is the sum of the components in (*b–e*). Data for observer G.P.W.

How reliable are the components in figure 3*b–e*, particularly the finer components in figure 3*d*,*e*? This question was addressed in several ways.

1. If the sequence of values forming a component were random, then there should be a lack of serial dependence. When first and second sample auto-correlation coefficients were calculated for each component from each observer, almost 90% of the coefficients were found to be significantly different from zero ($p < 0.02$; Appendix Ba).
2. When the finest non-zero component (figure 3*e*) was removed from the summed curve in figure 3*a*, or indeed when any of the other components was in turn removed, the fit of the summed curve to the increment-threshold function was found to fail significantly (over all observers, $p \ll 0.0001$; Appendix Bb).

3. When 'significant' minima and maxima in the finer components were enumerated, more were obtained than would have been expected by chance (over all observers, $p < 0.001$; Appendix Bc).
4. When the experiment was repeated, under different stimulus conditions, the finer components were found to preserve their shapes (§ 6 and Appendix Bc).

It seems unlikely that the reliability of the components is an artefact of the decomposition procedure: when applied to simple theoretical increment-threshold functions with a few strict minima and maxima (sinewave, sawtooth and bowed-squarewave functions), the procedure reproduced these functions exactly; it did not generate spurious harmonics with more minima and maxima than in the original functions (Appendix Ac).

In the next and subsequent sections the components produced by the decomposition procedure are considered in relation to possible visual mechanisms. By its nature, the procedure cannot be used to determine whether components arise from the activity of several mechanisms operating at different orientation scales or from the activity of a single mechanism with an oscillating orientation sensitivity that mimics the superposed activity of simpler mechanisms. But, as is shown in § 6, when the stimulus time-course is changed, the coarse and finer components are affected differently, suggesting that they cannot be attributed to the activity of a single monolithic mechanism.

4. DISTRIBUTION OF ORIENTATION SPACINGS

To summarize the results of the decomposition analyses for the ten observers, a histogram based on the statistics of the orientation components was constructed, as follows. Each component (figure 3*b–e*) can be segmented at points where it has a minimum, a procedure that yields a set of 'bump'-shaped subcomponents. Each of these subcomponents can be interpreted as evidence of an interaction between signals from orientation-selective visual mechanisms with adjacent preferred orientations (Foster & Ward 1991), a notion discussed more fully later. The angular width of the subcomponent, in degrees say, would then correspond to the angle between the preferred orientations of these hypothesized mechanisms, that is, the orientation spacing. A histogram can be formed by counting at each orientation spacing the number of subcomponents with that spacing, both within and across components. This histogram does, however, overrepresent the finer subcomponents (there are 12 subcomponents in figure 3*e* and two in figure 3*b*). To make any departures from uniformity more obvious, the observed number of counts at each spacing t was therefore multiplied by $t/90°$. (This normalization also made easier a comparison with the Fourier amplitude spectrum of the increment-threshold function; Appendix Aa.)

Figure 4*a* shows the normalized number of subcomponents, averaged over the ten observers, plotted against orientation spacing for a criterion level of target detection $d' = 0.5$. There are three prominent clusters in the histogram at orientation spacings of *ca.* 10°–25°, 35°–50° and 90°. The shaded region marks 5–95% pointwise confidence intervals (Appendix Bd).

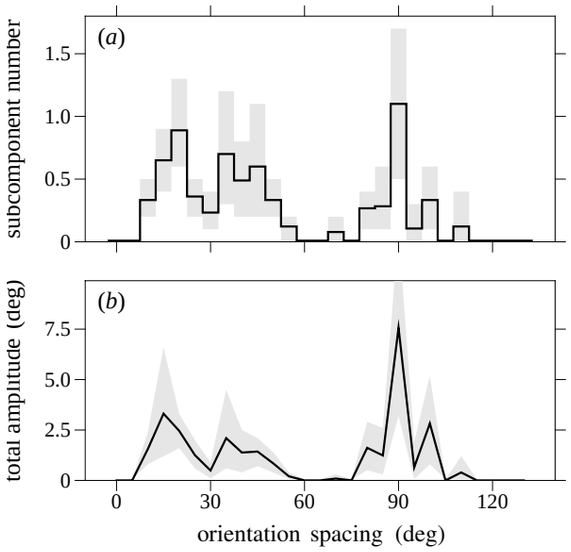

Figure 4. Estimates of number and amplitude of orientation subcomponents obtained in repeated-loess decompositions, as in figure 3. (*a*) Number of subcomponents at each orientation spacing. The three main clusters have orientation spacings of *ca.* 10°–25°, 35°–50° and 90°. (*b*) Total subcomponent amplitude at each orientation spacing. In both (*a*) and (*b*) the shaded regions mark 5–95% pointwise confidence intervals. The data were normalized to reveal departures from uniformity over orientation spacing. Data for ten observers.

The positions and profiles of the clusters were dependent, to some extent, on task difficulty: although the clusters at 10°–25° and 90° were fairly stable, the cluster at 35°–50° shifted towards smaller spacings when the detection criterion was lower ($d' = 0.2$), and towards larger spacings when the detection criterion was higher ($d' = 0.8$).

How does the amplitude of these subcomponents vary with orientation spacing? Figure 4*b* shows total subcomponent amplitude, summed within and across components, plotted against orientation spacing. The function was normalized in the same way as in figure 4*a* and was averaged over the ten observers. The shaded region marks 5–95% pointwise confidence intervals (calculated as in Appendix Bd). The variation of amplitude with orientation spacing was very similar to that for subcomponent number (and, as explained in Appendix Be, it provided a control on the way that subcomponents were counted). Subcomponent number and amplitude plots obtained from random increment-threshold functions are considered in Appendix Bf.

These data on orientation spacing do not give direct estimates of orientation bandwidths of the hypothesized orientation-selective mechanisms, but a previous approximate analysis (Foster & Ward 1991) suggested that a mechanism with an orientation spacing of 90° had an orientation bandwidth of about 60° (full width at half-height, not to be confused with the standard-deviation bandwidth used in the repeated-loess procedure). On that basis, mechanisms with orientation spacings of 35°–50° would have bandwidths of *ca.* 23°–33°, and those with

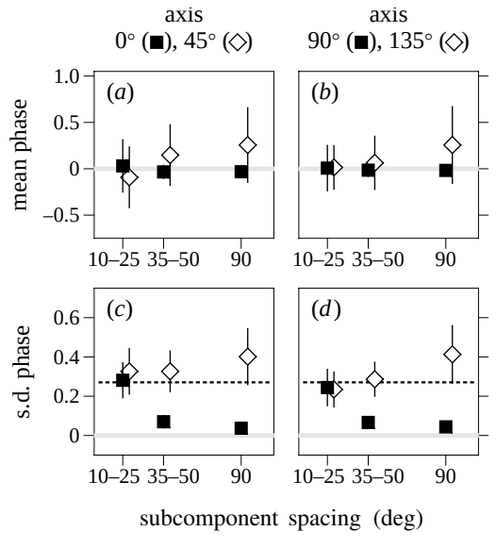

Figure 5. Congruence of preferred orientations. (*a*, *b*) Mean and (*c*, *d*) standard deviation of subcomponent phase with reference to axes at 0° (vertical), 45°, 90° and 135° for the three clusters of orientation subcomponents with orientation spacings of *ca*. 10°–25°, 35°–50° and 90°. (Symbols have been slightly offset horizontally for clarity.) Vertical bars indicate ±1 s.e.m., where sufficiently large. The broken line in (*c*, *d*) is the expected standard deviation for independent randomly distributed phases. Data for ten observers.

orientation spacings of 10°–25° would have bandwidths of *ca*. 7°–17°.

These values are not inconsistent with those found neurophysiologically in single-cell recordings from the primate cortex (Schiller *et al*. 1976; De Valois *et al*. 1982; Vogels & Orban 1990; Henry *et al*. 1994). For example, De Valois *et al*. (1982) found orientation bandwidths ranging from 8° to more than 100° in the macaque monkey striate cortex. Moreover, bandwidths of individual neurons may be temporally dependent, reflecting the differing dynamics of their excitatory and inhibitory inputs (Ringach *et al*. 1997).

5. CONGRUENCE OF PREFERRED ORIENTATIONS

Although the clusters in the histogram of subcomponent number against orientation spacing (figure 4*a*) can be explained by the action of groups of orientation-selective mechanisms with similar orientation spacings, it does not necessarily follow that the axes of the mechanisms are similarly aligned. What, then, are the preferred orientations of these mechanisms, and are they the same for all observers?

A convenient summary measure of alignment is the phase of each subcomponent, that is, the angle between the nearest minimum of the subcomponent and the vertical (or horizontal) divided by the angular width of the subcomponent. If the preferred orientations of the mechanisms were vertical or horizontal, then the mean phase over observers should be zero and the standard deviation should be small. Notice that having zero mean is not a sufficient condition for preferred orientations to be taken as the same, for a symmetric random distribution centred on the vertical or horizontal also has zero mean: a critical additional condition is that the standard deviation should be significantly smaller than that for the uniform distribution on the unit circle.

Figure 5 shows, for the ten observers, the mean (*a*,*b*) and standard deviation (*c*,*d*) of the phase of subcomponents near the vertical 0° and horizontal 90° (solid symbols), and, as a control, near the two oblique axes 45° and 135° (open symbols), for the three clusters of orientation subcomponents. The vertical bars indicate ±1 s.e.m., where sufficiently large. The broken line in figure 5*c*,*d* is the expected standard deviation for independent randomly distributed phases. For all axes, the mean phase (*a*,*b*) is indistinguishable from zero for each of the three subcomponent spacings, but the standard deviation (*c*,*d*), although close to zero for 35°–50° and 90°, increases markedly for 10°–25°, and is indistinguishable from that for a random variable. As expected, for the two oblique axes the standard deviation is indistinguishable from that for a random variable, for each of the three subcomponent spacings (cf. Regan & Price 1986).

If, as suggested, groups of orientation-selective mechanisms underlie this performance, then it seems that those with large and intermediate orientation spacings have a common alignment near the vertical and horizontal; but those with small orientation spacings have no common alignment, either near the vertical or horizontal or near the 45° oblique axes.

What determines the axis of preferred orientation? It is known that both visual context, such as the frame surrounding the line-element display (Treisman 1985), and gravity (Marendaz *et al*. 1993) affect the direction and magnitude of the vertical–oblique asymmetry in line-element search. For example, in experiments with observers supine, so that vestibular and somatosensory cues were very small, the asymmetry was found to be absent (Marendaz *et al*. 1993; but see Doherty & Foster 1998). In addition, in experiments with observers seated in a non-pendular centrifuge, so that the direction of the perceived gravito-inertial axis was altered, the direction of the asymmetry shifted appropriately (Stivalet *et al*. 1995).

These vestibular, proprioceptive and somatosensory orientation cues presumably affect only mechanisms with large and intermediate orientation spacings (Marendaz *et al*. 1993); the apparently haphazard alignment of those mechanisms with small spacings may simply represent a natural, independent, random variation in the sampling characteristics of individual neurons or groups of neurons (Das & Gilbert 1997).

6. DIFFERENTIAL EFFECTS OF DISPLAY DURATION

The time for which the line-element display was available for viewing was very short. Recall that it lasted for 40 ms, and after a blank interval of 60 ms a masking field was presented. Would more time for effective viewing influence the balance of activity of these hypothesized orientation-selective mechanisms? To answer this question, the duration of the blank interval between the line-element display and the mask—the interstimulus interval (ISI)—was increased to 180 ms, the energy in the stimulus therefore remaining the same, and the orientation increment-threshold functions redetermined for two observers (A.C. and S.W.).

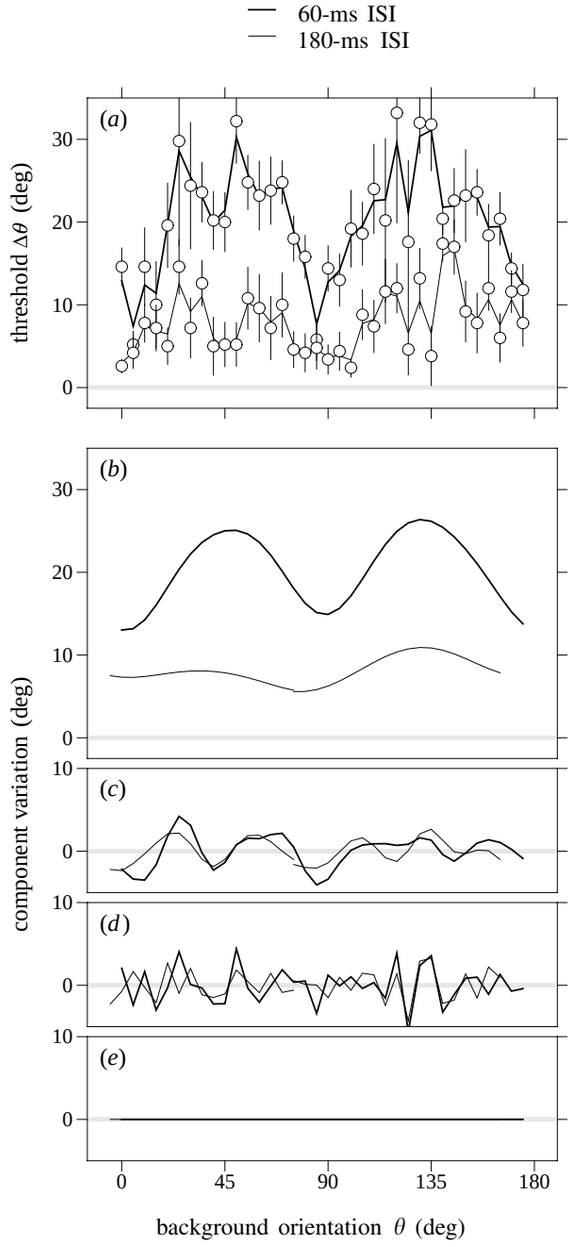

Figure 6. Effect of stimulus time-course. (*a*) Orientation increment-threshold functions for line-element detection and (*b*–*d*) decompositions into orientation components for intervals between the line-element display and masking field (ISIs) of 60 ms (thick line) and 180 ms (thin line). The 180-ms components have been shifted leftwards by 5° over the interval 0°–90° and by 10° over the interval 90°–180°. Data for observer A.C. Other details as in figure 3.

Figure 6 shows, for observer A.C., increment-threshold functions (*a*) and the results of decomposition analyses (*b*–*d*) for ISIs of 60 ms (thick line) and 180 ms (thin line; after a correcting shift leftwards by 5° over the interval 0°–90° and by 10° over the interval 90°–180°). For this observer both decompositions terminated at the third component.

For the ISI of 180 ms, thresholds were lower than for the ISI of 60 ms, which might be expected. But, it seems mainly due to a reduction in the amplitude of the coarse component (figure 6*b*): the amplitudes of the finer components (figure 6*c*,*d*) were similar (see also Doherty & Foster 1996*b*), as were their variations with background-element orientation, which *inter alia* provided a control on their reproducibility (Appendix Bc). A similar pattern of performance was obtained for observer S.W. For both observers the ratio of coarse- to fine-component amplitudes was approximately halved with the increase in ISI.

This shift in balance of apparent activity might be interpreted as evidence of the visual system performing a rudimentary 'coarse-to-fine' analysis of orientation information (Watt 1987; Hughes *et al*. 1996), although the possibility cannot be excluded that mechanisms with 90° orientation spacings still make a contribution to orientated-line detection at longer effective display durations but one which is isotropic. The effect of ISI does, however, vary from observer to observer (L. M. Doherty & D. H. Foster 1998, unpublished observations) and data would need to be obtained from a larger pool of observers and with more systematic variation in ISI before this result could be generalized.

7. ORIENTATION COMPONENTS AND DETECTION MECHANISMS

The notion that multiple groups of orientation-selective mechanisms underlie observed detection performance depends on several results from the analysis: (i) the decompositions of orientation increment-threshold functions from individual observers into distinct orientation components; (ii) the formation of clusters in the distribution of orientation subcomponent spacings averaged over observers; (iii) the different phase dependencies of subcomponents from different clusters; and (iv) the different amplitude dependencies of subcomponents from different clusters under changes in effective display duration. None of the analysis involved any specific assumptions about the nature of the detection process. How, then, might an orientation subcomponent arise from an interaction between signals from orientation-selective mechanisms with adjacent preferred orientations, as was suggested in § 4?

Consider how detection by just the coarse orientation-selective mechanisms varies with the anticlockwise rotation of the whole stimulus display. First, when the background elements are vertical and the target element is oblique (tilted anticlockwise), mechanisms whose preferred orientations are horizontal are activated strongly by the target element and only weakly by the background elements. The signal-to-noise ratio (SNR) for these mechanisms is high, and threshold is therefore low. (The mechanisms whose preferred orientations are vertical are activated strongly by the background elements and give a low SNR.) Next, when the background elements are oblique and the target element is horizontal, mechanisms whose preferred orientations are vertical or horizontal are activated strongly by the background elements. The SNR for each is low, and threshold is therefore high. Finally, when the background elements are horizontal and the target element is oblique, the SNR for mechanisms whose preferred orientations are vertical is high, and threshold is therefore low. In this way, the

positions of the threshold minima locate the preferred orientations of the mechanisms. Notice that detection is best at (or near to) the maximum of one mechanism's response, not where it is changing most rapidly, as in classical orientation acuity (cf. Regan & Beverley 1985).

This scheme, proposed in Foster & Ward (1991) to explain the vertical-oblique asymmetry in line-element search (Treisman & Souther 1985), can be regarded as an example of a more general scheme proposed by Treisman & Gormican (1988) in which an oblique (or tilted) line element is coded as a vertical line element with an additional feature marking the nature of the deviation. More quantitative analyses of target-detection performance based on signal-to-noise calculations for approximately orthogonal orientation-selective filters have been given elsewhere (a first-order approximation in Foster & Ward (1991) and an explicit computational model in Westland & Foster (1995)); such filters need not be assumed to act directly on the retinal image but possibly at some higher level (cf. Found & Müller 1997).

Interactions of this kind could occur between mechanisms with preferred orientations spaced more closely than 90°, thus accounting for the intermediate and fine fluctuations in the increment-threshold functions shown in figures 2, 3 and 6. Whether, like coarse orientation-selective mechanisms, intermediate and fine mechanisms have counterparts in the statistical components of real-world images (Baddeley & Hancock 1991) is not immediately clear; intermediate or finer mechanisms may, however, account for categorical effects revealed in some orientated-line search tasks (Wolfe *et al*. 1992).

8. NOISE ALONG THE OBLIQUE AXES

A different explanation of the orientation dependence of orientated-line detection has been proposed (Rubenstein & Sagi 1990) in which mechanisms responding to oblique line elements are assumed to be more noisy than those responding to vertical (or horizontal) line elements. The assumption of greater internal noise along the oblique axes (e.g. Mansfield 1974; Orban *et al*. 1984) has been invoked in some explanations of the classical oblique effect (Appelle 1972; Essock 1980). The size of this noise can be estimated by measuring how performance depends on the amount of external noise introduced into the stimulus (Barlow 1957). In such a study of orientation acuity with gratings and two-dimensional, band-pass-filtered spatial noise (Heeley *et al*. 1997), it was found that neither a reduced sampling density nor increased internal noise along a 45° oblique axis was sufficient to account for the measured oblique effect.

As to the present data, an explanation based on greater internal noise along the oblique axes is difficult to reconcile with (i) the presence of minima, not maxima, in some intermediate orientation components near background-element orientations of 45° and 135°, and (ii) the constancy of the standard deviation of the phase of the finest subcomponents with respect to axes at 0°, 45°, 90° and 135°. Yet the possibility of a more complex variation of internal noise with orientation cannot be excluded: expressed at multiple scales, it might provide an account of the various structures in the orientation increment-threshold function analysed here.

We thank H. B. Barlow, J. J. Koenderink, C. R. Loader, D. Lowe, L. T. Maloney, B. W. Silverman and C. K. I. Williams for helpful advice, and R. J. Baddeley, L. M. Doherty, T. S. Meese, M. G. A. Thomson, C. K. I. Williams and J. M. Wolfe for critical comments on the manuscript. Support was provided by the Wellcome Trust, grant no. 039958, and by the Defence Evaluation and Research Agency (formerly the Defence Research Agency), UK, contract no. D/ER1/9/4/2098/008.

REFERENCES

Ahissar, M. & Hochstein, S. 1997 Task difficulty and the specificity of perceptual learning. *Nature* **387**, 401–406.

Andrews, D. P. 1967 Perception of contour orientation in the central fovea. I. Short lines. *Vision Res*. **7**, 975–997.

Appelle, S. 1972 Perception and discrimination as a function of stimulus orientation: the "oblique effect" in man and animals. *Psychol. Bull*. **78**, 266–278.

Baddeley, R. J. & Hancock, P. J. B. 1991 A statistical analysis of natural images matches psychophysically derived orientation tuning curves. *Proc. R. Soc. Lond*. B **246**, 219–223.

Barlow, H. B. 1957 Increment thresholds at low intensities considered as signal/noise discriminations. *J. Physiol*. **136**, 469–488.

Beck, J. & Ambler, B. 1972 Discriminability of differences in line slope and in line arrangement as a function of mask delay. *Percept. Psychophys*. **12**, 33–38.

Bergen, J. R. & Julesz, B. 1983 Parallel versus serial processing in rapid pattern discrimination. *Nature* **303**, 696–698.

Chatfield, C. 1989 *The analysis of time series: an introduction*. London: Chapman & Hall.

Cleveland, R. B., Cleveland, W. S., McRae, J. E. & Terpenning, I. 1990 STL: a seasonal-trend decomposition procedure based on loess. *J. Off. Statist*. **6**, 3–73.

Cleveland, W. S. 1979 Robust locally weighted regression and smoothing scatter-plots. *J. Am. Statist. Ass*. **74**, 829–836.

Cleveland, W. S. 1993 *Visualizing data*. Summit, NJ: Hobart Press.

Das, A. & Gilbert, C. D. 1997 Distortions of visuotopic map match orientation singularities in primary visual cortex. *Nature* **387**, 594–598.

De Valois, R. L., Yund, E. W. & Hepler, N. 1982 The orientation and direction selectivity of cells in macaque visual cortex. *Vision Res*. **22**, 531–544.

Diggle, P. J. 1990 *Time series. A biostatistical introduction*. Oxford: Clarendon Press.

Doherty, L. M. & Foster, D. H. 1995 Detection of orientated line targets in very sparse displays. *Perception* **24**(Suppl.), 132.

Doherty, L. M. & Foster, D. H. 1996*a* Anisotropy in orientated-line-target detection at high and low luminance contrast. *Perception* **25**(Suppl.), 54.

Doherty, L. M. & Foster, D. H. 1996*b* Variation of detectability of orientated line targets with effective viewing duration. *Invest. Ophthalmol. Vis. Sci*. **37**, S295.

Doherty, L. M. & Foster, D. H. 1998 Orientational anisotropy in line-target detection with and without a gravitational reference for orientation. *Perception* **28**(Suppl.), 54.

Efron, B. & Tibshirani, R. J. 1993 *An introduction to the bootstrap*. New York: Chapman & Hall.

Essock, E. A. 1980 The oblique effect of stimulus identification considered with respect to two classes of oblique effects. *Perception* **9**, 37–46.

Fan, J. & Gijbels, I. 1996 *Local polynomial modelling and its applications*. London: Chapman & Hall.

Foster, D. H. & Bischof, W. F. 1991 Thresholds from psychometric functions: superiority of bootstrap to incremental and probit variance estimators. *Psychol. Bull*. **109**, 152–159.

Foster, D. H. & Ward, P. A. 1991 Asymmetries in orientated-line detection indicate two orthogonal filters in early vision. *Proc. R. Soc. Lond.* B **243**, 75–81.

Found, A. & Müller, H. J. 1997 Local and global orientation in visual search. *Percept. Psychophys.* **59**, 941–963.

Grambsch, P. M., Randall, B. L., Bostick, R. M., Potter, J. D. & Louis, T. A. 1995 Modeling the labeling index distribution: an application of functional data analysis. *J. Am. Statist. Ass.* **90**, 813–821.

Green, D. M. & Swets, J. A. 1966 *Signal detection theory and psychophysics*. New York: Wiley.

Hastie, T. J. & Tibshirani, R. J. 1990 *Generalized additive models*. London: Chapman & Hall.

Heeley, D. W., Buchanan-Smith, H. M., Cromwell, J. A. & Wright, J. S. 1997 The oblique effect in orientation acuity. *Vision Res.* **37**, 235–242.

Henry, G. H., Michalski, A., Wimborne, B. M. & McCart, R. J. 1994 The nature and origin of orientation specificity in neurons of the visual pathways. *Prog. Neurobiol.* **43**, 381–437.

Hirsch, J. & Hylton, R. 1982 Limits of spatial-frequency discrimination as evidence of neural interpolation. *J. Opt. Soc. Am.* **10**, 1367–1374.

Hughes, H. C., Nozawa, G. & Kitterle, F. 1996 Global precedence, spatial frequency channels, and the statistics of natural images. *J. Cogn. Neurosci.* **8**, 197–230.

Javadnia, A. & Ruddock, K. H. 1988 The limits of parallel processing in the visual discrimination of orientation and magnification. *Spatial Vis.* **3**, 97–114.

Julesz, B. & Schumer, R. A. 1981 Early visual perception. *A. Rev. Psychol.* **32**, 575–627.

Karni, A. & Sagi, D. 1991 Where practice makes perfect in texture discrimination: evidence for primary visual cortex plasticity. *Proc. Natn. Acad. Sci. USA* **88**, 4966–4970.

Macaulay, F. R. 1931 *The smoothing of time series*. New York: National Bureau of Economic Research Inc.

Mansfield, R. J. W. 1974 Neural basis of orientation perception in primate vision. *Science* **186**, 1133–1135.

Mardia, K. V. 1972 *Statistics of directional data*. London: Academic Press.

Marendaz, C., Stivalet, P., Barraclough, L. & Walkowiac, P. 1993 Effect of gravitational cues on visual search for orientation. *J. Exp. Psychol. Hum. Percept. Perform.* **19**, 1266–1277.

Meigen, T., Lagrèze, W.-D. & Bach, M. 1994 Asymmetries in preattentive line detection. *Vision Res.* **34**, 3103–3109.

Neisser, U. 1967 *Cognitive psychology*. Englewood Cliffs, NJ: Prentice-Hall.

Nothdurft, H. C. 1991 Texture segmentation and pop-out from orientation contrast. *Vision Res.* **31**, 1073–1078.

Orban, G. A., Vandenbussche, E. & Vogels, R. 1984 Human orientation discrimination tested with long stimuli. *Vision Res.* **24**, 121–128.

Ramsay, J. O. & Dalzell, C. J. 1991 Some tools for functional data analysis. *J. R. Statist. Soc.* B **53**, 539–572.

Regan, D. & Beverley, K. I. 1985 Postadaptation orientation discrimination. *J. Opt. Soc. Am.* A **2**, 147–155.

Regan, D. & Price, P. 1986 Periodicity in orientation discrimination and the unconfounding of visual information. *Vision Res.* **26**, 1299–1302.

Rice, J. A. & Silverman, B. W. 1991 Estimating the mean and covariance structure nonparametrically when the data are curves. *J. R. Statist. Soc.* B **53**, 233–243.

Ringach, D. L., Hawken, M. J. & Shapley, R. 1997 Dynamics of orientation tuning in macaque primary visual cortex. *Nature* **387**, 281–284.

Rubenstein, B. S. & Sagi, D. 1990 Spatial variability as a limiting factor in texture-discrimination tasks: implications for performance asymmetries. *J. Opt. Soc. Am.* A **7**, 1632–1643.

Sagi, D. & Julesz, B. 1985 "Where" and "what" in vision. *Science* **228**, 1217–1219.

Sagi, D. & Julesz, B. 1987 Short-range limitation on detection of feature differences. *Spatial Vis.* **2**, 39–49.

Schiller, P. H., Finlay, B. L. & Volman, S. F. 1976 Quantitative studies of single-cell properties in monkey striate cortex. II. Orientation specificity and ocular dominance. *J. Neurophysiol.* **39**, 1320–1333.

Schoups, A. A. & Orban, G. A. 1996 Interocular transfer in perceptual learning of a pop-out discrimination task. *Proc. Natn. Acad. Sci. USA* **93**, 7358–7362.

Silverman, B. W. 1986 *Density estimation for statistics and data analysis*. London: Chapman & Hall.

Simonoff, J. S. 1996 *Smoothing methods in statistics*. New York: Springer.

Spencer, J. 1904 On the graduation of the rates of sickness and mortality. *J. Inst. Actuaries* **38**, 334–343.

Stivalet, P., Marendaz, C., Barraclough, L. & Mourareau, C. 1995 Effect of gravito-inertial cues on the coding of orientation in pre-attentive vision. *J. Vestibular Res.* **5**, 125–135.

Treisman, A. 1985 Preattentive processing in vision. *Comput. Vis. Graph. Image Proc.* **31**, 156–177.

Treisman, A. & Gormican, S. 1988 Feature analysis in early vision: evidence from search asymmetries. *Psychol. Rev.* **95**, 15–48.

Treisman, A. & Souther, J. 1985 Search asymmetry: a diagnostic for preattentive processing of separable features. *J. Exp. Psychol. Gen.* **114**, 285–310.

Treisman, A. M. & Gelade, G. 1980 A feature-integration theory of attention. *Cogn. Psychol.* **12**, 97–136.

Treisman, A. M., Sykes, M. & Gelade, G. 1977 Selective attention and stimulus integration. In *Attention and performance VI* (ed. S. Dornic), pp. 333–361. Hillsdale, NJ: Lawrence Erlbaum.

Vogels, R. & Orban, G. A. 1990 How well do response changes of striate neurons signal differences in orientation: a study in the discriminating monkey. *J. Neurosci.* **10**, 3543–3558.

Watt, R. J. 1987 Scanning from coarse to fine spatial scales in the human visual system after the onset of a stimulus. *J. Opt. Soc. Am.* A **4**, 2006–2021.

Westheimer, G. 1984 Line-separation discrimination curve in the human fovea: smooth or segmented? *J. Opt. Soc. Am.* A **1**, 683–684.

Westheimer, G. 1990 Simultaneous orientation contrast for lines in the human fovea. *Vision Res.* **30**, 1913–1921.

Westheimer, G. & McKee, S. P. 1977 Spatial configurations for visual hyperacuity. *Vision Res.* **17**, 941–947.

Westland, S. & Foster, D. H. 1995 Optimized model of orientated-line-target detection using vertical and horizontal filters. *J. Opt. Soc. Am.* A **12**, 1617–1622.

Wolfe, J. M. 1992 "Effortless" texture segmentation and "parallel" visual search are *not* the same thing. *Vision Res.* **32**, 757–763.

Wolfe, J. M. 1994 Visual search in continuous, naturalistic stimuli. *Vision Res.* **34**, 1187–1195.

Wolfe, J. M., Friedman-Hill, S. R., Stewart, M. I. & O'Connell, K. M. 1992 The role of categorization in visual search for orientation. *J. Exp. Psychol. Hum. Percept. Perform.* **18**, 34–49.